Sustainable Production Scheduling with On-Site Intermittent Renewable Energy and Demand-Side Management: A Feed-Animal Case Study

Mohamed Habib Jabeur, Sonia Mahjoub, Cyril Toublanc

▶ **To cite this version:**

Mohamed Habib Jabeur, Sonia Mahjoub, Cyril Toublanc. Sustainable Production Scheduling with On-Site Intermittent Renewable Energy and Demand-Side Management: A Feed-Animal Case Study. Energies, 2023, 16 (14), pp.5433. 10.3390/en16145433 . hal-04273795

HAL Id: hal-04273795
https://oniris.hal.science/hal-04273795

Submitted on 7 Nov 2023

HAL is a multi-disciplinary open access archive for the deposit and dissemination of scientific research documents, whether they are published or not. The documents may come from teaching and research institutions in France or abroad, or from public or private research centers.

L'archive ouverte pluridisciplinaire **HAL**, est destinée au dépôt et à la diffusion de documents scientifiques de niveau recherche, publiés ou non, émanant des établissements d'enseignement et de recherche français ou étrangers, des laboratoires publics ou privés.

Distributed under a Creative Commons Attribution 4.0 International License

energies

MDPI

Article

Sustainable Production Scheduling with On-Site Intermittent Renewable Energy and Demand-Side Management: A Feed-Animal Case Study

Mohamed Habib Jabeur [1,*], Sonia Mahjoub [2] and Cyril Toublanc [3]

[1] Oniris, INRAE, STATSC, 44300 Nantes, France
[2] Oniris, Nantes University, LEMNA, CS 82225, 44322 Nantes, France
[3] Oniris, Nantes University, CNRS, GEPEA, UMR 6144, F-44000 Nantes, France
* Correspondence: mohamed-habib.jabeur@oniris-nantes.fr; Tel.: +33-617619991

Abstract: By shifting towards renewable energy sources, manufacturing facilities can significantly reduce their carbon footprint. This environmental issue can be addressed by developing sustainable production through on-site renewable electricity generation and demand-side management policies. In this study, the energy required to power the manufacturing system is obtained from different energy sources: the conventional grid, on-site renewable energy, and an energy storage system. The main objective is to generate a production schedule for a flexible multi-process and multi-product manufacturing system that optimizes the utilization and procurement of electricity without affecting the final demand. A mathematical programming model is proposed to minimize both the total production costs and energy costs, considering a time-of-use pricing policy and an incentive-based program. The uncertainty in renewable energy generation, specifically under the worst-case scenario, is taken into account and the model is transformed into a robust two-stage optimization model. To solve this model, a decomposition approach based on a genetic algorithm is applied. The effectiveness of the proposed model and algorithm is tested on a real industry case involving feed-animal products. A sensitivity analysis is conducted by modifying problem parameters. Finally, a comparison with the nested Column and Constraint Generation algorithm is performed. The obtained results from these analyses validated the proposed model and algorithm.

Keywords: production scheduling; demand-side management; onsite renewable; uncertainty; robust optimization; genetic algorithm

check for updates

Citation: Jabeur, M.H.; Mahjoub, S.; Toublanc, C. Sustainable Production Scheduling with On-Site Intermittent Renewable Energy and Demand-Side Management: A Feed-Animal Case Study. *Energies* **2023**, *16*, 5433. https://doi.org/10.3390/en16145433

Academic Editor: Surender Reddy Salkuti

Received: 8 June 2023
Revised: 4 July 2023
Accepted: 14 July 2023
Published: 17 July 2023

Copyright: © 2023 by the authors. Licensee MDPI, Basel, Switzerland. This article is an open access article distributed under the terms and conditions of the Creative Commons Attribution (CC BY) license (https://creativecommons.org/licenses/by/4.0/).

1. Introduction

Climate change presents a major concern, and there is a growing recognition among governments and companies of the need to take concrete actions to address the impact of the global carbon footprint. The industrial sector, being one of the largest energy consumers and greenhouse gas (GHG) emitters worldwide, faces significant pressure to reduce its carbon footprint. According to [1], approximately 24% of global GHG emissions are attributed to industrial energy consumption, while industrial processes contribute to about 5% of these emissions. The primary source of GHG emissions in industrial activities is the utilization of fossil fuels for electricity generation. In this way, improving the energy efficiency of the manufacturing process is being recognized as a promising pathway towards sustainable manufacturing, offering both environmental benefits and opportunities for cost savings [2]. Achieving cleaner production involves enhancing the energy efficiency of process equipment and incorporating energy and resource efficiency considerations into production scheduling [3]. Integrating an energy management system into production scheduling can not only improve economic and environmental performance, but it also can aid in balancing the supply and demand of electricity during peak periods without the need for additional infrastructure investments. The reduction of energy consumption during

peak periods can be achieved through the implementation of a demand response (DR) program, which is recognized as a highly promising aspect of demand-side management (DSM) [4]. DR refers to the alteration of electricity usage by end users in response to changes in electricity prices over time [4,5]. It serves as an effective means to maintain a balance between supply and demand [6]. Various solutions and mechanisms are encompassed within DR, including real-time pricing, critical peak pricing, and time-of-use (TOU) pricing, among others [7]. TOU pricing is particularly popular as a demand response mechanism, as it incentivizes electricity consumers to shift their power consumption from high-priced peak periods to low-priced off-peak periods [8]. Manufacturing industries can benefit significantly from this pricing scheme by shifting their production activities away from peak periods, leading to substantial energy cost savings [7]. Numerous studies have addressed production scheduling under TOU electricity pricing. Ref. [9] developed an optimization model for process industries with batch and continuous stages to determine optimal production scheduling under TOU tariff structures. Ref. [8] investigated the implementation of a TOU-based electricity demand response strategy for a sustainable manufacturing system with multiple machines and buffers. They formulated a mathematical model to minimize total electricity consumption and cost while adhering to production targets. Ref. [10] expanded on their previous study by conducting monotonicity analysis on machine and buffer parameters. Ref. [11] established a Nonlinear Integer Programming (NIP) model based on a novel buffer inventory policy to reduce electricity consumption during peak periods without compromising the manufacturing system. Ref. [12] relaxed the throughput constraint and integrated potential production losses into the objective function of the NIP model. Ref. [7] proposed a multi-objective optimization model to address the job-shop scheduling problem under TOU electricity prices.

Another way to meet excessive peak electricity demands and reduce greenhouse gas (GHG) emissions is through the utilization of renewable energy resources. These cleaner resources provide a viable strategy for achieving energy cost reduction while simultaneously reducing carbon emissions. Incorporating renewable energy sources like solar and wind energy into the manufacturing process enables a significant reduction in carbon emissions, supporting the development of sustainable manufacturing practices [13]. However, it should be noted that renewable energy is subject to intermittency and fluctuates with weather variations. The inherent uncertainty in renewable energy resources can introduce inaccuracies in scheduling solutions. To address these challenges, the implementation of energy storage systems (ESS) has emerged as a promising solution [14]. ESS can store excess energy generated by renewable sources during periods of high production and make it available during times when renewable energy production is low or unavailable. In recent years, there have been several studies focusing on the utilization of on-site renewable energy generation systems to power industrial plants. For instance, ref. [15] considered the use of on-site renewable energy as support for implementing diverse demand response (DR) programs in manufacturing facilities. The authors proposed a stochastic programming model to maximize annual utility savings by selecting appropriate on-site renewable energy systems (RES). In [16], the use of renewable energy through wind turbines integrated with the electrical grid was investigated within the context of dynamic production scheduling. They formulated a mixed-integer linear programming (MILP) model to minimize the expected total energy cost. Similarly, ref. [17] developed a multi-stage stochastic model to address production planning in a manufacturing system powered by on-site and grid renewable energy. Ref. [18] presented a two-stage stochastic optimization method to study the scheduling problem in a flow-shop system with an on-site wind power supply. The integration of on-site renewable generation and energy storage systems in the context of flow-shop scheduling has also been studied [14]. The authors formulated a two-stage multi-objective stochastic program to determine the optimal production schedule and energy supply decisions. Furthermore, ref. [19] established a mathematical programming model to address the multi-process production scheduling problem by considering on-site renewable energy supply, grid power supply, on-site energy storage systems, and different

demand-side management (DSM) policies. They formulated a two-stage robust optimization framework to incorporate uncertainties related to renewable energy and generate a robust production schedule. Additionally, [20] developed a dynamic approach to manufacturing system scheduling that aligns machine power with the availability of renewable energy without compromising production and market requirements.

By incorporating renewable energy sources, conventional grid energy, and ESS into the production scheduling model, it is possible to achieve sustainable production practices by reducing the environmental impact of manufacturing processes, such as carbon emissions, and promoting the use of clean and renewable resources. Additionally, the hypothesis proposes that this integration can lead to cost savings in both production and energy consumption, indicating the potential economic benefits of implementing such a system. In this context, this research paper focuses on addressing the production scheduling problem in a flexible multi-process and multi-product manufacturing system that is powered by on-site renewable energy, conventional grid energy, and an on-site energy storage system (ESS). The objective of this study is to minimize both the global production cost and energy costs under different DR policies, including TOU pricing policies and an incentive-based program involving power consumption reduction requests from the utility company. To tackle the uncertainties associated with renewable energy supply, a two-stage robust optimization framework is developed. The problem is formulated as a mixed-integer linear programming (MILP) model. To solve this complex problem, a decomposition approach based on a genetic algorithm is employed. The model outputs of this study include flexible multi-processes, inventory levels, back-orders, on-site renewable energy, ESS dynamics, and the consumption amounts of both conventional and renewable energy under different DR and incentive-based programs. The effectiveness of the proposed model is tested on a real industry case of animal-feed products. The main contributions of this work are:

- Developing a comprehensive model that addresses the production scheduling problem in a flexible multi-process and multi-product manufacturing system.
- Incorporating a two-stage robust optimization framework to handle uncertainties in renewable energy supply and employing a decomposition approach based on a genetic algorithm to solve the complex optimization problem.
- Performing numerical experiments, sensitivity analysis, and a comparison with the nested Column and Constraint (CCG) algorithm to show the effectiveness of both the model and algorithm.

The rest of the current paper is organized as follows. Section 2 describes the considered problem and presents the mathematical model. In Section 3, the different resolution approaches are developed. Section 4 reveals the results through numerical experiments on a real-world case study and other numerical experiments. Finally, conclusions and future work directions are presented in Section 5.

2. Problem Description and Mathematical Model

2.1. Problem Description and Mathematical Model

This paper focuses on investigating the implementation of sustainable production scheduling in a flexible multi-process and multi-product manufacturing system. The system considered in this study involves both batch and continuous processes, with buffers incorporated between adjacent processes. These buffers play a crucial role in ensuring smooth production flow and minimizing disruptions.

In the context of the animal-feed industry, which relies heavily on energy-intensive machines for thermal and mechanical operations, energy cost becomes a significant concern. To address this issue, renewable energy sources are explored as a promising alternative to achieve sustainable production with reduced carbon emissions. The manufacturing system in this study procures energy from three different sources: the conventional grid, on-site renewable energy generation, and an ESS (e.g., see Figure 1). On-site renewable energy is utilized for power production activities and charges the ESS. The ESS is employed to efficiently manage the intermittency of renewable energy by storing excess energy for later

use. The primary objective of this research is to develop a production scheduling model that optimizes energy utilization while ensuring no impact on the final delivery demand for each product. To achieve this, a mathematical programming model is proposed. The model aims to minimize both the total production cost and energy cost, while respecting production throughput requirements and adhering to energy supply policies.

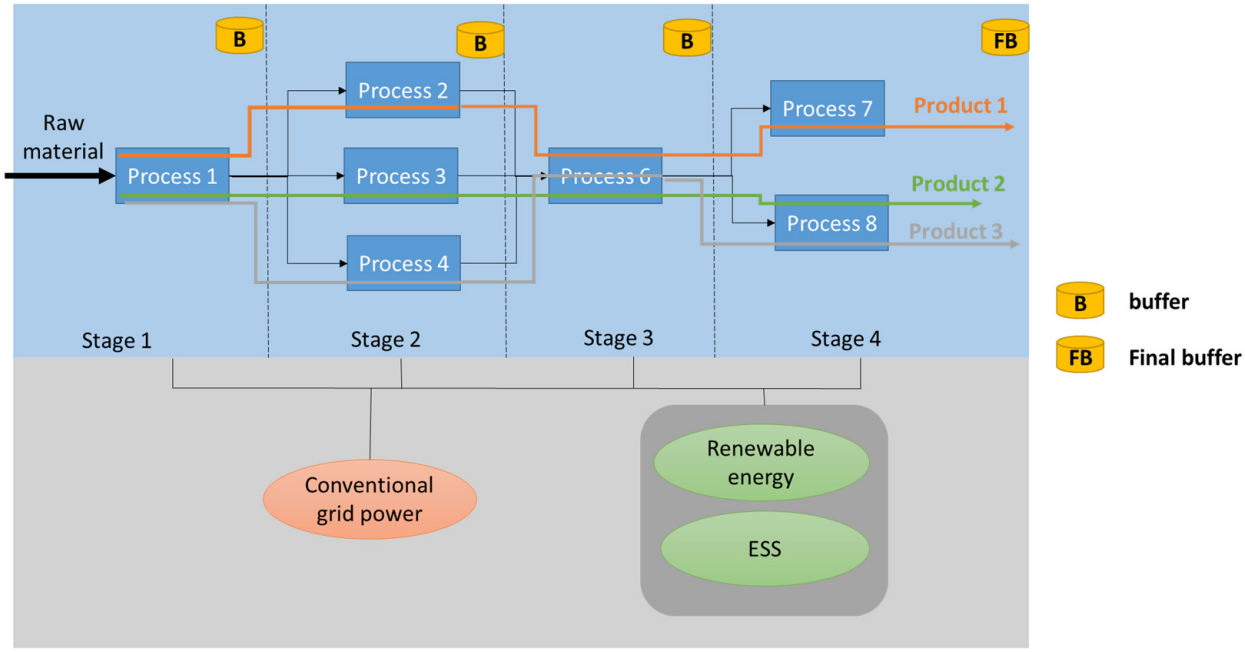

Figure 1. Reference context: manufacturing system with on-site RES and ESS.

2.2. Mathematical Model

In this section, the production scheduling problem, considering energy supply decisions, is formulated as a mixed-integer linear programming (MILP) model. To enhance the clarity of the model presentation, the sets, parameters, and decision variables are listed in Appendix A.

2.2.1. Objective Functions

The aim of the proposed MILP is to simultaneously minimize:

1-Production costs (Equation (1)), denoted as C_{prod}, which is calculated as the sum of the buffering cost, the holding cost of final products, and back-ordered costs. It is important to note that the processing cost is not considered in this study, as it does not affect the production cost regardless of changes in the production schedule.

$$C_{prod} = \sum_{t \in T} \sum_{p \in P} \sum_{i \in I_p} C_p^y \cdot y_{i,p,t} + C_p^q \cdot q_{i,p,t} + C_p^v \cdot v_{i,p,t} \quad (1)$$

2-Energy costs (Equation (2)), denoted as C_{prod}, which considers the expenses associated with the charging and discharging dynamics of the ESS, the conventional energy cost, on-site renewable energy costs, and incentives for accepting power consumption reduction requests.

$$C_E = \sum_{t \epsilon T} \left(c_t^+ \cdot r_t^+ + c_t^- \cdot r_t^- + g_t^{(1)} \cdot e_t^{(1)} + g_t^{(2)} \cdot e_t^{(2)} - g_t^+ \cdot a_t \right) \quad (2)$$

Hence, the objective function is expressed as follows:

$$C = \min(C_{prod} + C_E) \quad (3)$$

2.2.2. Production Scheduling Constraints

The production scheduling optimization problem is subject to: (1) demand satisfaction constraints, (2) flow balance constraints, (3) production and inventory capacity constraints, (4) production continuity constraints, (5) batch process constraints, and (6) non-negativity constraints, which are described hereafter.

1-Demand satisfaction constraints: constraints (4) express the relation between the final product, inventory level, and backorders and final demand.

$$\alpha_p \cdot x_{i,p,t} + q_{i,p,t-1} - q_{i,p,t} - v_{i,p,t-1} + v_{i,p,t} = D_{i,p,t},\ \forall\, t \,\epsilon\, T,\ \forall\, p \,\epsilon\, \delta,\ \forall\, i \,\epsilon\, I_p \tag{4}$$

2-Flow balance constraints: constraint sets (5) and (6) model the production and buffering of product i in process p at period t, respectively.

$$\alpha_p \cdot x_{i,p,t} = \sum_{p'=1}^{P} b_{i,\,p,p'} \cdot x^{(1)}_{i,p,p',t} + x^{(2)}_{i,p,t},\ \forall\, i \in I_p,\ \forall\, p \in P,\ \forall\, t \in T, \tag{5}$$

$$y_{i,p,t} = \sum_{p'=1}^{P} b_{i,p,p'} \cdot y^{(1)}_{i,p,p',t} + y^{(2)}_{i,p,t},\ \forall\, i \in I_p,\ \forall\, p \in P,\ \forall\, t \in T, \tag{6}$$

Constraints (7) and (8) ensure the flow equilibrium for process p at period t for production and buffering, respectively.

$$x_{i,p,t} = \sum_{p'=1}^{P} b_{i,p',p} \left(x^{(1)}_{i,p',p\ ,t-1} + y^{(1)}_{i,p',p\ ,t-1} \right),\ \forall\, i \in I_p\ ,\ p \in \{2, .., |P|\}\ ,\ \forall\, t \in T \tag{7}$$

$$y_{i,p,t} = x^{(2)}_{i,p,t} + y^{(2)}_{i,p,t-1}\ , \forall\, i \in I_p,\ \forall\, p \in P,\ \forall\, t \in T, \tag{8}$$

3-Production and inventory capacity constraints: the cycle time capacity for each process is modeled in (9), where $\frac{1}{T_P}$ represents the number of products that can be processed on process p in one period.

$$\sum_{i=1}^{I_p} x_{i,p,t} \leq \frac{1}{T_P}\ ,\ \forall\, p\ \in P,\ \forall\, t \in T \tag{9}$$

The buffering capacity of process p is defined in (10), and the maximum level of final product inventory is expressed in (11).

$$\sum_{i \epsilon I_p} y_{i,p,t} \leq N_p,\ \forall\, i\ \in I_p,\ \forall\, p\ \in P,\ \forall\, t \in T \tag{10}$$

$$\sum_{i \epsilon I_p} q_{i,p,t} \leq I_{max},\ \forall\, p \in \delta,\ \forall\, t \in T, \tag{11}$$

4-Production continuity constraints: constraint (12) ensures the production continuity of all the processes during 24 h, and constraint (13) imposes that the final inventory at period T must be equal to the initial inventory.

$$y_{i,p,T} = y0_{i,p},\quad \forall\, i\ \in I_p,\ \forall\, p\ \in P \tag{12}$$

$$q_{i,p,T} = I0_{i,p},\quad \forall\, i\ \in I_p,\ \forall\, p\ \in \delta \tag{13}$$

5-Batch process constraints: The integration of these constraints in the mathematical model guarantee a feasible production schedule. Constraint (14) ensures that the incoming flow to the batch process should be greater than the lot size and lower than the production capacity of this process. The setup constraint is expressed in Constraint (15), where M is a big parameter that imposes an upper bound on the production quantity. The capacity production of batch process is defined in Constraint (16).

$$K_p \leq \sum_{p'=1}^{P} b_{i,p',p} \left(x^{(1)}_{i,p',p\ ,t} + y^{(1)}_{i,p',p\ ,t} \right) \leq \frac{1}{T_P},\ \forall\, i \in I_p\ ,\ \forall\, p \in \theta,\ \forall\, t \in T, \tag{14}$$

$$\sum_{i \epsilon I_p} x_{i,p,t} \leq M \cdot Se_{p,t}\ , \forall\ i \in I_p\ \ , \forall\ p \in \theta, \forall\ t \in T \tag{15}$$

$$T_p \cdot \sum_{i \epsilon I_p} x_{i,p,t} + f_{p,t} \cdot Se_{p,t} \leq 1\ , \forall\ i \in I_p\ \ , \forall\ p \in \theta, \forall\ t \in T \tag{16}$$

6-Non-negativity: Constraints (17) and (18) provide variable types.

$$x_{i,p,t},\ y_{i,p,t},\ x^{(1)}_{i,p,p',t},\ x^{(2)}_{i,p,t},\ y^{(1)}_{i,p,p',t},\ y^{(2)}_{i,p,t},\ q_{i,p,t},\ v_{i,p,t} \geq 0, \forall\ i \in I_p\ \ , p \in P\ , \forall\ p' \in P, \forall\ t \in T \tag{17}$$

$$Se_{p,t} = 0 or\ \ Se_{p,t} = 1\ , \forall\ t \in T, \forall\ p \in \theta \tag{18}$$

2.2.3. The Energy Policies Constraints

The energy policies constraints under TOU electricity prices are described as follows.

1-ESS constraint: The charge/discharge dynamics of the ESS are defined in (19)–(23). Lower and upper bounds on the amount of energy stored in an ESS at period t are imposed by (19). Constraint (20) defines the state of charge of the ESS at period t, which is equal to the state of charge of the ESS over the previous period, s_{t-1} plus the amount of power energy to charge the ESS during the period t, r_t^+ minus the amount of power energy to discharge the ESS at the period t, r_t^-. The charge and discharge capacities of the ESS are expressed in (21) and (22), respectively. Constraint (23) imposes that the final state of charge of the ESS at period T must be the same as the initial charge level.

$$S_{min} \leq s_t\ \leq S_{max}\ , \forall t \in T \tag{19}$$

$$s_t = s_{t-1} + \eta^+ \cdot r_t^+ - r_t^- \frac{1}{\eta^-}\ , \forall t \in T \tag{20}$$

$$r_t^+ \leq R,\ \forall t \in T \tag{21}$$

$$r_t^- \leq R,\ \forall t \in T \tag{22}$$

$$s_T = S_0 \tag{23}$$

2-DSM policies and energy sources: The dynamic of the energy management system is defined in (24)–(26). Constraint (24) ensures that the total energy requirements for the production processes are satisfied, where the right-hand side represents the energy supplied by the on-site renewable energy, the grid energy, and the ESS. Constraint (25) models the distribution of the generated on-site renewable energy between consumed energy and the ESS. This constraint is formulated as an inequality in order to avoid the risk associated with the uncertainty of the renewable energy. Constraint (26) models the conventional energy grid supply considering the DSM policy of power consumption reduction requests.

$$\sum_{i=1}^{Ip} \sum_{p \epsilon P} E_p \cdot x_{i,p,t} = r_t^- + e_t^{(2)} + e_t^{(1)},\ \forall t \in T \tag{24}$$

$$G_t \geq e_t^{(1)} + r_t^+,\ \forall\ t \in T \tag{25}$$

$$e_t^{(2)} + R_t\ \cdot a_t \leq R_t, \forall t \in T \tag{26}$$

3-Non-negativity: non-negativity and binary requirements are modeled in constraint (27).

$$s_t, r_t^+, r_t^-, e_t^{(2)}, e_t^{(1)} \geq 0,\ a_t\ \epsilon\ \{0,1\},\ \forall t \in T \tag{27}$$

2.3. The Transformed MILP under Uncertain RES: Robust Approach

Uncertainty poses a significant challenge in industrial processes. Operational decisions need to be made considering economic and energy-related factors that are highly time-sensitive, such as final demand and electricity prices. In this paper, the fluctuating nature of renewable energy is addressed in the proposed optimization approach to enhance the model's performance. Inspired by [19], this study incorporates a robust approach to integrate uncertainty regarding on-site RES into the MILP model. The objective of the robust optimization methodology is to determine the "best uncertainty-immunized" solution under the worst-case scenario for each uncertain parameter [21,22].

2.3.1. Uncertain RES and Budget-Uncertainty Set

In this section, it is supposed that the generation of renewable energy on-site belongs to uncertainty set $G_t \in \mu_1$. Let G_t be the uncertain parameter and $\hat{G}_t$ be the nominal value for available energy. The uncertain parameter G_t can deviate from the mean value $\hat{G}_t$ within the interval $\left[-\sigma_t^{(1)}, \sigma_t^{(1)}\right]$, where $o_t^{(1)+}, o_t^{(1)-}$ represent the scaled deviations. Then, the uncertainty set μ_1 can be modeled as follow:

$$\mu_1 = \left\{ G_t = \hat{G}_t + \Delta o_t^{(1)} \cdot \sigma_t^{(1)}, \ \forall t \in T \right.$$

$$\Delta o_t^{(1)} = o_t^{(1)+} - o_t^{(1)-}, \ \forall\, t \in T$$

$$0 \le o_t^{(1)+} \le 1, \ \forall t \in T$$

$$0 \le o_t^{(1)-} \le 1, \ \forall\, t \in T$$

$$\left. \sum_{t \epsilon T} o_t^{(1)+} + o_t^{(1)-} \le \Gamma^{(1)} \right\}$$

μ_1 is usually denominated as a budget-uncertainty set because of the user-specific parameter $\Gamma^{(1)}$, also called budget of uncertainty, which imposes an upper bound on the variation of the uncertain parameter to avoid very pessimistic solutions [22]. In this study, it is supposed that $0 \le \Gamma^{(1)} \le T$, where T represents the number of periods.

2.3.2. Robust Optimization Model

The goal of robust optimization is to define the production scheduling under the worst-case scenario. Thus, this approach aims to determine the best solution that remains feasible for any realization of the uncertain parameter within the uncertainty set [22]. The integration of the budget-uncertainty set of RES into the deterministic MILP leads to the following two-stage robust model:

$$\min_{x} C^T x + \max_{g_1} \min_{a,e} d^T a + f_1^T (e_1 + e_2) \tag{28}$$

$$A \cdot x \le b \tag{29}$$

$$Bx + Ha + J_1 e_1 + J_2 e_2 \le h + g_1 \tag{30}$$

$$x, \ e_1, e_2 \ge 0\,, \tag{31}$$

where g_1 represents the vector corresponding to renewable energy availability, G_t. x is the variables vector related to production planning: $x_{i,p,t}$, $y_{i,p,t}$, $x^{(1)}_{i,p,p',t}$, $x^{(2)}_{i,p,t}$, $y^{(1)}_{i,p,p',t}$, $y^{(2)}_{i,p,t}$, $q_{i,p,t}$, $v_{i,p,t}$ and $Se_{p,t}$. e_1 denotes the continuous energy variables vector related to renewable energy consumption. The vector e_2 includes the other continuous energy decision variables,

$s_t, r_t^+, r_t^-, e_t^{(2)}$. The vector a is a binary decision variables vector related to power reduction consumption requests. C, d,f_1, present the appropriate matrix and vectors related to the objective function. Finally, b, h, A, B, H, J_1, J_2 are the appropriate matrix and vectors related to the model constraints. The objective function C expressed in (28) is formulated as Min-Max-Min problem. Production Constraints (4)–(17) are reflected in (29). Energy Constraints (19)–(26) are reflected in (30). Finally, domains variables (18) and (27) are reflected in (31).

3. Solution Approaches

The two-stage robust optimization model (28)–(31) is designed to optimize the manufacturing scheduling under the worst-case scenario of RES output. This model, known as Min-Max-Min, represents a highly complex problem (NP-Hard problem) that cannot be efficiently solved using classical optimization techniques. To address this challenge, decomposition algorithms like Benders decomposition and the Column and Constraint Generation (C and CG) algorithm based on duality offer promising solutions, enabling the formulation of tractable solutions. These algorithms decompose the robust optimization model into a Master Problem (MP) and a Sub-problem (SP). They dynamically generate constraints with recourse variables in the primal space [23] based on a given uncertainty realization. To ensure convergence within a few iterations, an accurate exchange of information between the MP and the SP is essential. In other words, an optimal global solution must be obtained for each problem. Despite their promising capabilities, these algorithms have several inherent limitations. Firstly, their computational complexity can be a significant drawback, particularly for large-scale problems, as solving both the MP and SP iteratively can result in a substantial computational burden. Secondly, achieving convergence of the algorithm can be challenging, requiring optimal global solutions for both the MP and the SP within a reasonable number of iterations. Failure to converge may render the algorithm impractical or unable to provide optimal solutions. Additionally, the effectiveness of these iterative algorithms can be sensitive to the problem's structure, making them less suitable for certain problem types. Moreover, highly complex models with intricate constraints and decision variables may pose challenges for the performance of these algorithms. In addition, the presence of binary variables in the proposed model prevents direct dualizing of the SP. To deal with this and to ensure a feasible solution, we propose a decomposition genetic approach to solve the robust optimization model. The proposed approach aims to decompose the robust optimization model into two distinct problems: an MP and an SP. The objective is to identify the worst-case scenario within the SP using the genetic algorithm and determine the best production schedule within the MP. We use the genetic algorithm to solve the SP due to its ability to explore a wide search space and identify near-optimal solutions efficiently. In addition, the genetic algorithm's ability to handle mixed-variable optimization problems makes it a suitable choice for our robust optimization model.

3.1. Decomposition Approach

This decomposition strategy allows us to effectively handle the uncertainty and consider the robustness of the optimization solution. By solving both problems and exchanging information between them, we aim to find the best possible production schedule that is immune to the worst-case scenario of uncertain parameters. The Sub-problem (SP) is specifically tailored to handle the worst-case scenario, primarily focusing on the energy aspect of the model where RES are subject to uncertainty. The objective of the SP is twofold: to maximize the costs associated with RES power and simultaneously minimize other energetic costs. By finding the worst-case scenario of the SP, we can better understand the impact of the uncertain RES on the overall energy costs. The MP is dedicated to optimizing production planning across the scheduling horizon. It takes into account the solution obtained from the SP and aims to optimize the production schedule by considering various factors such as demand, capacities, and production costs. The objective of the MP is to find the most efficient and cost-effective production plan given the uncertainties and con-

straints. The proposed resolution approach combines the resolution of these two problems to address the robustness of the optimization problem. By solving the SP and exchanging information with the MP, we can find the production schedule to account for uncertainties and make it more resilient. This framework ensures a holistic approach to address the robustness and optimality of the production scheduling problem under uncertainty. In the following sections, we will provide a detailed description of the construction and implementation of this framework.

3.1.1. The Sub-Problem: Genetic Algorithm

In the SP, the objective is to obtain a feasible solution that is robust under the worst-case scenario. To achieve this, we focus on the max-min decision level and isolate the energy variables from the production variables. The Sub-problem is defined as follows:

SP:

$$\max_{g_1} \min_{a,e} d^T a + f_1^T (e_1 + e_2) \tag{32}$$

$$Bx + Ha + J_1 e_1 + J_2 e_2 \leq h + g_1 \tag{33}$$

$$x,\ e_1, e_2 \geq 0,\ a\ \epsilon\ \{0,1\} \tag{34}$$

To solve this problem, the duality approach [19,24] can be employed. However, it is important to note that the duality approach has its limitations. In cases where weak duality holds, the approach may result in a bounded solution and fail to provide unique optimal solutions. Additionally, the duality approach is not suitable for solving non-convex programs. Furthermore, when dealing with large-scale problems that involve extensive sets of variables and constraints, the problem becomes intractable. The computational complexity increases significantly, making it challenging to obtain efficient and timely solutions using the duality approach. Given these limitations, we use the genetic algorithm (GA) to overcome these challenges. Pointed out by [25], the genetic algorithm can be applied to convert the max-min problem into a min problem and find a robust solution. The GA is a meta-heuristic algorithm inspired by the principle of natural evolution. It is commonly used for solving complex optimization problems [26]. In this paper, we consider that the GA maintains a population P, which represents all the potential scenarios. This population evolves over iterations, converging towards the worst-case scenario and enabling the identification of a robust solution. The population P consists of individuals that represent solutions in the context of g_1. Each individual in P corresponds to a specific solution, and its performance under the worst-case scenario is evaluated using the objective function $f(g_1)$. The objective function $f(g_1)$ defined in Equation (35) quantifies the performance or fitness of a solution based on its worst-case outcome. It takes into account various factors, such as costs, constraints, and performance metrics, relevant to the problem at hand. By evaluating the objective function for each solution in P, we can assess the worst-case performance of each individual solution in relation to the considered scenario g_1.

$$f(g_1) = \min_{a,e} d^T a + f_1^T (e_1 + e_2) \tag{35}$$

S.T (33) and (34)

The algorithm rewards the largest $f(g_1)$ and the best solution is determined by the chromosome with the highest value of $f(g_1)$. In the context of solving complex optimization problems using a genetic algorithm (GA), chromosomes are typically represented by binary, integer, or real numbers. The choice of an appropriate chromosome representation plays a crucial role in enhancing the efficiency of the GA [27]. In the proposed GA, the chromosomes are composed of positive multiple deviations, $o_t^{(1)+}$, and the negative multiple deviations, $o_t^{(1)-}$, defined previously in Section 2.3.1. Each gene within the chromosome is an integer that takes a value of either 0 or 1. The specific coding of the solution using this chromosome representation is illustrated in Figure 2.

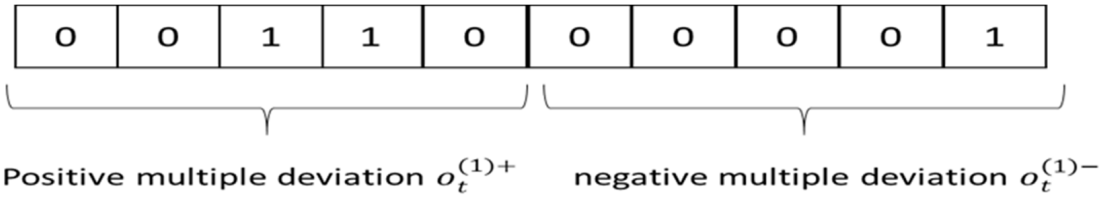

Figure 2. Solution coding for five periods scheduling.

By utilizing this coding scheme, the GA can explore and evolve the population of chromosomes, searching for the most optimal combination of genes that leads to higher values of the objective function $f(g_1)$. The genetic operators, such as selection, crossover, and mutation, are applied to manipulate and modify the chromosomes in order to improve their fitness and converge towards the best solution.

Hence, the steps of the proposed GA are presented in Algorithm 1:

Algorithm 1: Genetic-algorithm (x)

(1) Initialise first population P (i = 0)
(2) While (i < max number of generation):
(3) For individual $\mathbf{g}_1$ in population P:
Evaluate fitness function $f(\mathbf{g}_1)$
(4) i = i + 1
(5) Create next population P(i) by selection, crossover and mutation.
(6) End while
(7) Calculate $\mathbf{g}_1$ which has the biggest fitness
(8) Return $\mathbf{g}_1$

3.1.2. Master Problem

At this stage, the objective is to determine the optimal production scheduling and energy management system operations while considering the worst-case scenario of g_1, which has been identified in the SP. To accomplish this, the Master Problem can be reformulated as follows in MP1:

MP1:

$$\varphi = \min_{x} C^T x + \eta \tag{36}$$

$$Ax \leq b \tag{37}$$

$$Bx + Ha + J_1 e_1 + J_2 e_2 \leq h + g_1, \tag{38}$$

$$\eta \geq d^T a + f_1^T (e_1 + e_2), \tag{39}$$

$$x,\ e_1, e_2 \geq 0,\ a\ \epsilon\ \{0,1\}, \tag{40}$$

In this formulation, the objective function φ aims to minimize the cost production cost while incorporating the worst-case scenario component η, which represents the energy-related costs. The decision variables x correspond to the production planning and operations. The constraints in MP1 include the production-related constraints (37) to ensure that the production plan satisfies capacity, demand, and other production requirements. Additionally, the new constraint (38) is introduced to incorporate the worst-case scenario g_1 obtained from the SP. These constraints ensure that the energy management system operations align with the constraints imposed by the worst-case scenario. The constraint (39) ensures that η captures the energy-related costs, considering the decision variables a, e_1, and e_2. By reformulating the Master Problem as MP1, the optimization process seeks to find the optimal values for the decision variables x, e_1, and e_2, considering the worst-case scenario of g_1. The objective is to minimize the overall cost while ensuring feasibility and

robustness in production scheduling and energy management system operations. Since the MP and the SP are strongly connected through the constraint (24), the exchange of information between the two problems is facilitated by variables x and g_1. In order to solve the SP, it is necessary to have a feasible solution for x, which represents the production scheduling. Similarly, to solve the MP, a feasible solution for g_1, which corresponds to the worst-case scenario, is required. The SP focuses on determining a feasible solution under the worst-case scenario. By considering the given values of x, the SP evaluates the corresponding values of g_1 that satisfy the constraints and represent the worst-case energy scenario. This information is then transferred to the MP to ensure that the production scheduling and energy management decisions take into account the robustness provided by the worst-case scenario. Therefore, both problems should be solved in a coordinated manner. To initiate this process, we begin with a feasible solution for g_1, which represents a feasible scenario. This selection of g_1 is crucial as it determines the production scheduling and energy management decisions that optimize performance under the worst-case conditions. Algorithm 2 is applied to solve the proposed model and to obtain the best solution of the robust scheduling model:

Algorithm 2: Resolution algorithm ()

(1) $\mathbf{g_1} = \hat{G}_t$,
(2) Solve MP1
(3) Find $\hat{\mathbf{x}}$, $\hat{\mathbf{e}_1}, \hat{\mathbf{e}_2}, \hat{\mathbf{a}}$,
(4) $\mathbf{g_1}* = \text{genetic} - \text{algorithm}\ (\hat{\mathbf{x}})$
(5) $\mathbf{g_1}^{(v)} = \mathbf{g_1}*$
(6) Resolve MP1
(7) Return $\mathbf{x}*$, $\mathbf{e}_1*, \mathbf{e}_2*, \mathbf{a}*$, $\mathbf{g_1}*$ and $\varphi*$

Figure 3 shows the flow chart of the decomposition approach based on the genetic algorithm.

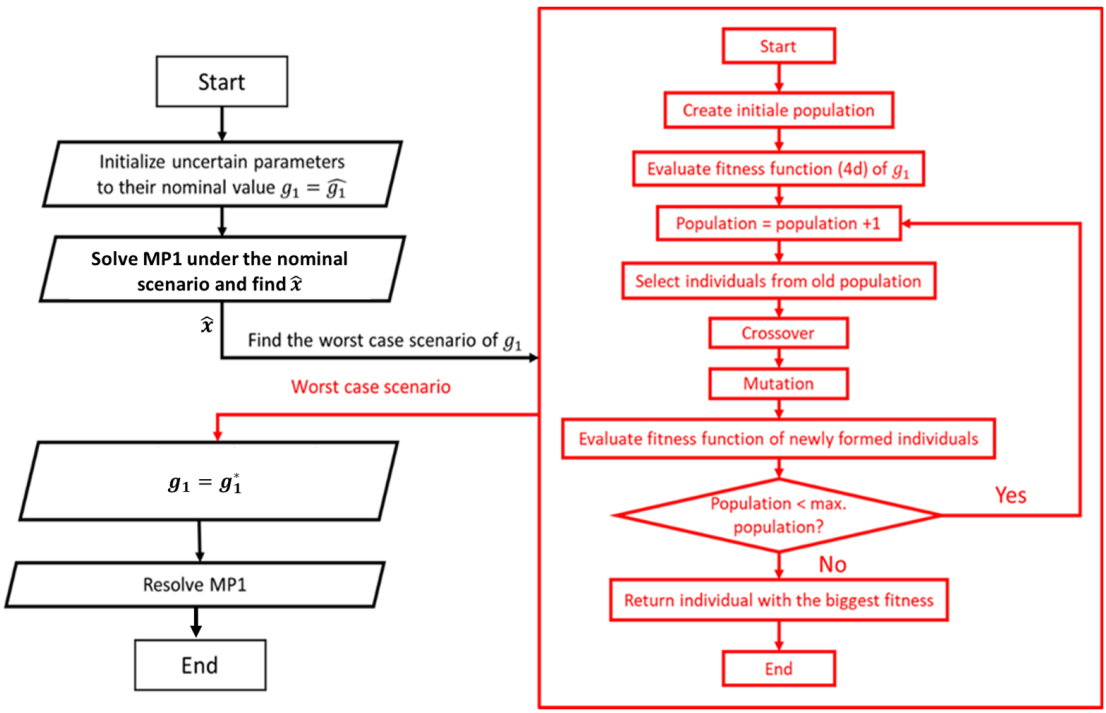

Figure 3. Flow chart of the proposed approach.

4. Computational Experiments

In this section, a real-world case study is conducted on an animal-feed manufacturing plant to achieve two objectives: (1) illustrate the proposed robust scheduling model, and

(2) assess and compare the performance of different resolution approaches. The proposed model is solved using PULP 2.4.1, a library for linear programming in Python 3.8. The resolution approaches are implemented in Python 3.8. The computation times required to solve the model and execute the resolution approaches are measured in CPU seconds, providing insights into the computational efficiency of each method.

4.1. Manufacturing Process Description

This section looks at the case study of an animal-feed manufacturing company based in Nantes, France. The animal-feed manufacturing plant is highly automated and energy-intensive. Its production process involves several stages (Figure 4), including reception and preparation of raw materials, grinding to reduce particle size, dosage and mixing for formulation, granulation, and filtering to obtain the final products. The plant utilizes a combination of conventional grid power, photovoltaic panels, and an energy storage system to meet its electrical demand. This integrated energy system ensures a reliable and sustainable energy supply. By considering the material flow, production processes, and energy supply system, the proposed robust optimization framework can be applied to optimize production scheduling and energy management decisions for the improved efficiency and performance of the plant.

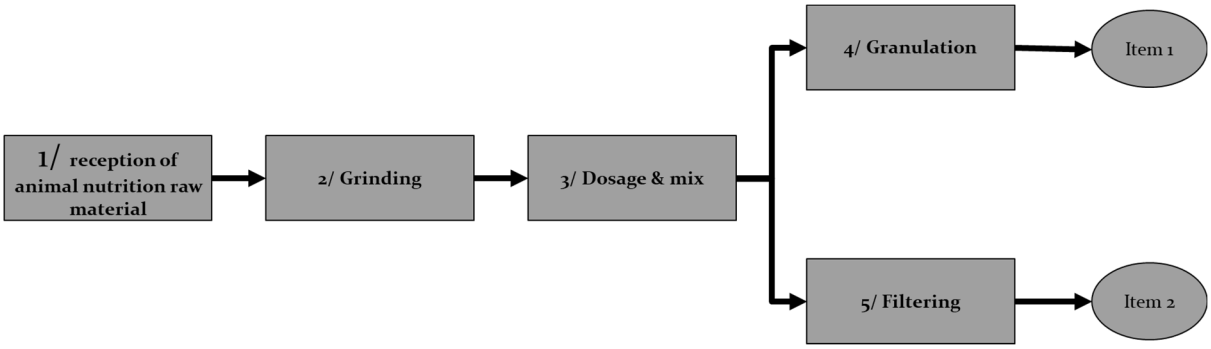

Figure 4. Manufacturing processes.

4.2. Input Data

In this research paper, the focus is on production scheduling for a day-ahead horizon, which is divided into eight periods representing three hours each. The production parameters presented in the rest of this paper are adjusted from Tecaliman [28], a technological research center dedicated to the mastery of processes historically used in animal nutrition. The desired demand for different product types is specified in Table 1, while Table 2 provides information on the characteristics of the production processes. To evaluate the costs associated with inventory management, a unit inventory cost of 10 EUR/ton is considered for the final products. Additionally, a backorder cost of 0.1 EUR/kg is included in the analysis. Notably, the backorder cost is assumed to be significantly higher during the last period to ensure that all demand is fulfilled by the end of the scheduling horizon. The initial inventories for the final products are set as follows: $I0_{1,4} = I0_{1,5} = I0_{2,4} = I0_{2,5} = 0$. Furthermore, the maximum capacity for the inventory of final products is set at I_{max} =150 tons. Table 3 provides energy parameters used in the analysis, which have been adjusted from [17,19] studies. The on-peak period comprises periods five and six, while the off-peak period consists of periods one, two, three, four, seven, and eight. The power consumption reduction requests (DSM) are set to $R_t = 3$ megawatt. To incentivize and motivate the reduction efforts, a financial incentive of $g_t^+ =$ EUR 500 per period is offered. The parameters related to the ESS are derived from [29] and are assigned the following values: $S_{min} = 500$ kWh, $S_{max} = 2$ MWh, $S_0 = 500$ kwh, $R^+ = R^- = 150$ kWh, $\eta^+ = \eta^- = 0.9$ and $c^+ = c^- = 30$ EUR/MWh. The budget of uncertainty of renewable energy, denoted as $\Gamma^{(1)}$, is set to four. This parameter represents the allowable deviation or fluctuation in the renewable energy generation. It

quantifies the level of uncertainty that can be tolerated within the optimization model. Additionally, the French CO_2 emission factor associated with electricity consumption is approximately 0.1 kg/kWh. The genetic algorithm parameters used to find the worst-case scenario are presented as follows: size = 50, best_sample = 10, number of child = 2, generation_number = 20, mutation_chance = 10.

Table 1. Product demands (ton).

Parameters	t = 1	t = 2	t = 3	t = 4	t = 5	t = 6	t = 7	t = 8
$D_{1,4,t}$ (ton)	0	0	27	22	37	30	28	0
$D_{2,4,t}$ (ton)	0	0	5	3	4	9	7	0
$D_{1,5,t}$ (ton)	0	0	29	31	24	33	31	0
$D_{2,5,t}$ (ton)	0	0	3	6	8	6	7	0

Table 2. Process parameters.

Parameters	p = 1	p = 2	p = 3	p = 4	p = 5
c_p^y (EUR)	0.1	0.1	0.1	0.1	0.1
T_p (time/ton)	0.006	0.0075	0.009	0.008	0.008
α_p	1	1	1	1	1
N_p (ton)	125	125	125	0	0
$y0_{1,p}$ (ton)	15	15	15	0	0
$y0_{2,p}$ (ton)	15	15	15	0	0
E_p (MW/ton)	0.00114	0.008	0.003	0.028	0.001
Batch parameters	p = 1	p = 2	p = 3	p = 4	p = 5
K_t (ton)	-	-	3	-	-
f_t (time)	-	-	0.05	-	-

Table 3. Energy parameters: TOU prices and uncertain renewable energy.

Parameters	t = 1	t = 2	t = 3	t = 4	t = 5	t = 6	t = 7	t = 8
$g_t^{(1)}$ (EUR/MWh)	50	50	50	50	50	50	50	50
$g_t^{(2)}$ (EUR/MWh)	70	70	70	70	110	110	70	70
$\hat{G}_t$ (megawatt)	0	0	0.2	1.11	1.67	1.22	0.2	0
$\sigma_t^{(1)}$ (megawatt)	0	0	0.073	0.44	0.22	0.324	0.087	0

4.3. Results and Discussion on the Benchmark Case

The simulation of the proposed algorithm in the benchmark case, considering TOU prices and uncertain renewable energy, yielded a total cost of EUR 524.81. This cost consists of an energy cost component of EUR 354.16 and an inventory cost component of EUR 170.65. Furthermore, the CO_2 emissions associated with the production schedule were measured to be 714.2 kg. Figure 5 depicts the production schedule of raw material 1, illustrating the quantity of products processed at each stage. Figure 6 presents the corresponding inventory levels associated with this production schedule. The flow of the production schedule for product 1 is shown in Figure 7.

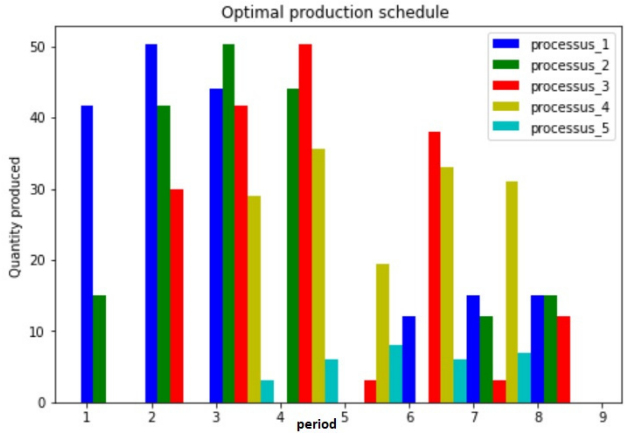

Figure 5. Best production schedule for product 1.

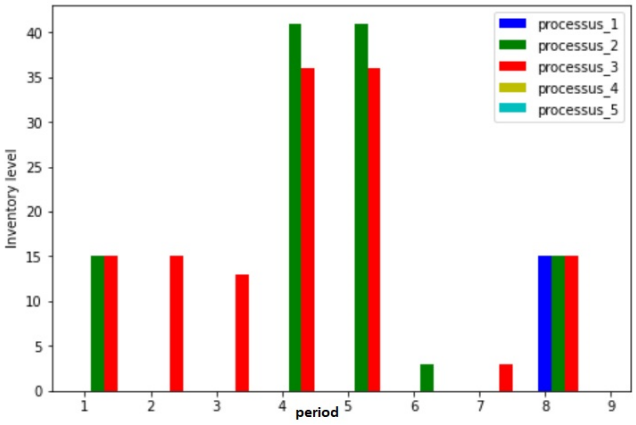

Figure 6. Product 1 inventory level.

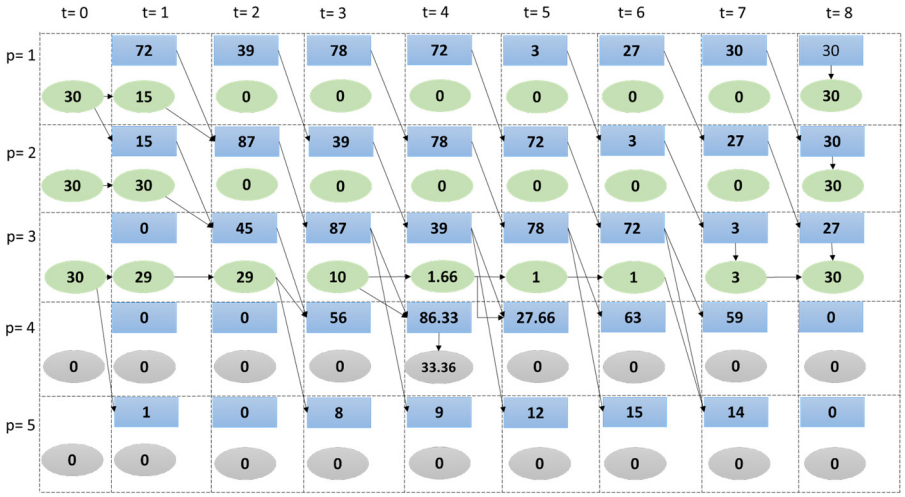

Figure 7. Best process flow (product 1).

The electrical energy plans related to the obtained production schedule are illustrated in Figure 8. It is evident that the electrical energy plans associated with the production schedule optimize the consumption of conventional energy during high-price periods, specifically periods five and six. Notably, there is no grid energy consumption during period five, indicating that a power consumption reduction request has been accepted. During this period, the energy demand is exclusively met by on-site renewable energy sources and the ESS. The operation of the ESS is dynamic and adheres to the capacity

constraints of the system (Figure 9). It undergoes charging during off-peak periods (periods two and three) when electricity prices are lower, and discharging occurs during on-peak periods (periods five and six) when prices are higher. This flexible utilization of the ESS optimizes energy management and reduces reliance on grid energy during peak hours.

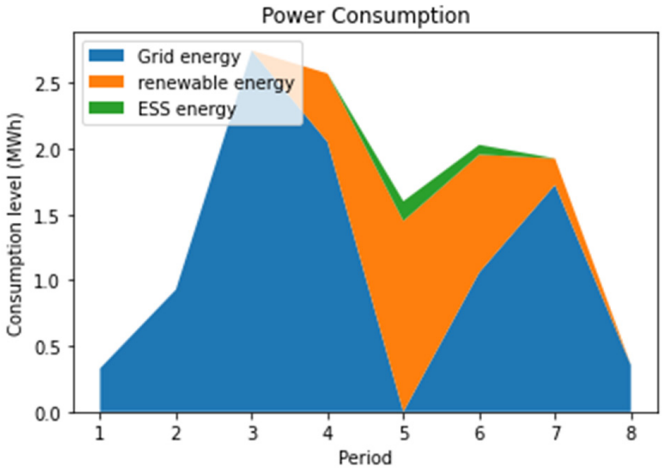

Figure 8. Electrical energy.

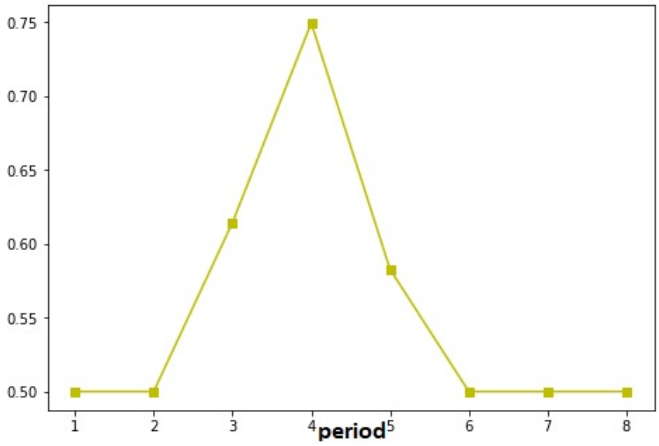

Figure 9. ESS operation dynamics.

The global distribution of energy consumption during the production scheduling horizon is illustrated in Figure 10. The analysis reveals that energy consumption is distributed across various sources. Conventional energy accounts for the majority share, representing 73.6% of the total energy consumption. Intermittent solar energy follows as the second highest contributor, accounting for 27.9%. The ESS contributes 1.8% of the total energy consumption. These findings indicate that the utilization of on-site renewable energy sources and the ESS significantly contribute to enhancing energy efficiency and flexibility within the manufacturing system. The integration of RES and ESS helps reduce reliance on conventional energy sources and promotes sustainability. It is important to note that this distribution is specific to the particular day of production analyzed in the study. The results are influenced by the available renewable electrical energy, which depends on the installed capacities of electricity production and storage on-site.

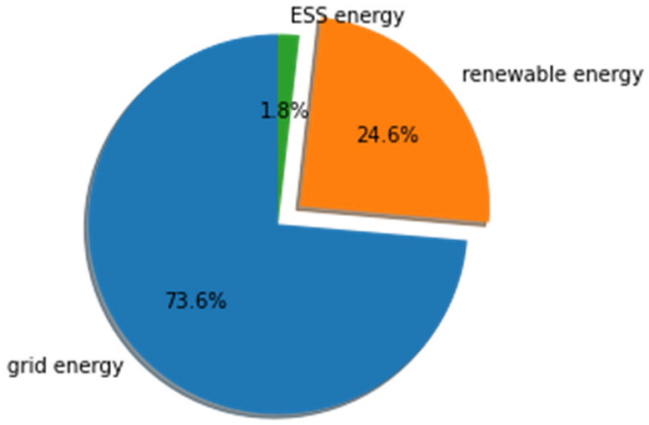

Figure 10. Distribution of energy consumption.

4.4. Sensitivity Analysis

The proposed approach in our study allowed us to conduct a comprehensive sensitivity analysis to assess the impact of various modifications on the study case. By systematically altering specific parameters, we were able to evaluate the robustness and effectiveness of our model in different scenarios. The following modifications were considered: (1) remove renewable energy; (2) perform partial clearing; (3) integrate uncertain spot prices instead of TOU prices; (4) modify on-peak periods; (5) modify budget of uncertainty; (6) modify time granularity.

4.4.1. Scheduling Model under TOU Prices without Renewable Energy

In this case, the proposed model and algorithms are tested under only the TOU pricing policy without considering a renewable energy system. Then, the electrical grid only powers the manufacturing system. The obtained results of this case show that the daily total cost is slightly increased compared to the previous scenario. However, the energy cost (EUR 1021) has drastically raised (three times more expensive). This is due to the high cost of grid energy. Thus, the rise of the energy bought from the grid leads to a considerable increase of CO_2 emissions (1248 kg). However, in the absence of on-site RES, the inventory cost (EUR 81) is reduced by 52% compared to the benchmark case and all the production processes are operated nonstop to satisfy the final demands. As a consequence, the request of power consumption reduction is not deployed in any period. The obtained results of this case show that incorporating renewable energy helps to save energy costs and then reduce CO_2 emissions. Furthermore, the results show the economic effectiveness achieved due to the production scheduling flexibility gained by incorporating renewable energy in implementing DSM policies.

4.4.2. Production Scheduling Model under Partial Energy Clearing

The objective of this experiment is to test the applicability of the model under a partial energy clearing. To do this, a limit level of energy consumption, β, is imposed and added to constraint (2 h) as follows:

$$e_t^{(2)} + R_t \cdot a_t \leq R_t + \beta$$

For β = 0.5 MWh, the total cost is EUR 1046.19, which is slightly reduced compared to the previous case and is ~100% higher than the one obtained in the benchmark case. The energy cost is EUR 473.254, which is higher by EUR 119.1, 33.6%, than the one obtained in the benchmark case. However, the inventory cost is EUR 572.93, which is significantly higher compared to the two previous cases. This rise of inventory cost is essentially due to the increase of inventory level to fulfill final demand.

4.4.3. Production Scheduling Model Considering Uncertainty about RES and Spot Prices

In this scenario, uncertainty about electricity prices is considered and integrated into the benchmarking model. Hence, the conventional energy price $g_t^{(2)}$ is based on uncertain spot prices and assumed to belong to a budget-uncertainty set μ_2 formulated as follow:

$$\left.\begin{array}{c} \mu_2 = \{g_t^{(2)} = \hat{g_t^{(2)}} + \Delta o_t^{(2)}.\sigma_t^{(2)} \\ \Delta o_t^{(2)} = o_t^{(2)+} - o_t^{(2)-} \quad \forall t \in T \\ 0 \le o_t^{(2)+} \le 1 \quad \forall t \in T \\ 0 \le o_t^{(2)-} \le 1 \quad \forall\, t \in T \\ \sum_{t \epsilon T} o_t^{(2)+} + o_t^{(2)-} \le \Gamma^{(2)} \end{array}\right\}$$

where $o_t^{(2)+}, o_t^{(2)-}$ capture, respectively, the positive and the negative multiples deviation from the nominal value. The total number of the multiples deviation must be controlled by a budget of uncertainty parameter $\Gamma^{(2)}$.

As a result, the transformed robust MILP under both RES and electricity price uncertainties takes the following form:

$$\min_{x} C^T x + \max_{g_1, g_2} \min_{a,e} d^T a + f_1^T e_1 + g_2 e_2 \tag{41}$$

$$A \cdot x \le b \tag{42}$$

$$Bx + Ha + J_1 e_1 + J_2 e_2 \le h + g_1 \tag{43}$$

$$x,\ e_1, e_2,\ a \epsilon \{0, 1\} \tag{44}$$

where g_2 represents the vector corresponding to spot prices, $g_t^{(2)}$.

In this simulation, the new model and the resolution methodology combining the C and GC algorithm and the genetic algorithm are tested using the following data:

- The budget of uncertainty of spot prices is set to $\Gamma^{(2)} = 5$.
- The uncertain spot price parameters during a springer's day are shown in Table 4 and Figure 11. The use of springer's day prices allows the elimination of the seasonality effect on the test results.

Table 4. Numerical results for case study instances.

Parameters	t = 1	t = 2	t = 3	t = 4	t = 5	t = 6	t = 7	t = 8
$g_t^{(2)}$	58.405	39.48	63.23	58.804	77.42	82.29	88.3055	85.99
$\sigma_t^{(2)}$	13.58	8.34	18.89	24.556	15.38	12.11	11.36	10

Figure 11 illustrates the spot price variation during eight periods in a spring day. It represents three different parts: the mean value of electricity spot price $\hat{g_t^{(2)}}$, the max value $\hat{g_t^{(2)}} + \sigma_t^{(2)}$, and the min value $\hat{g_t^{(2)}} - \sigma_t^{(2)}$. In this simulation, the total cost is equal to EUR 592.97, which is slightly higher than the benchmark case. The inventory and energy costs are also increased compared to the first case. The CO_2 emission is raised to attain 968.5 kg.

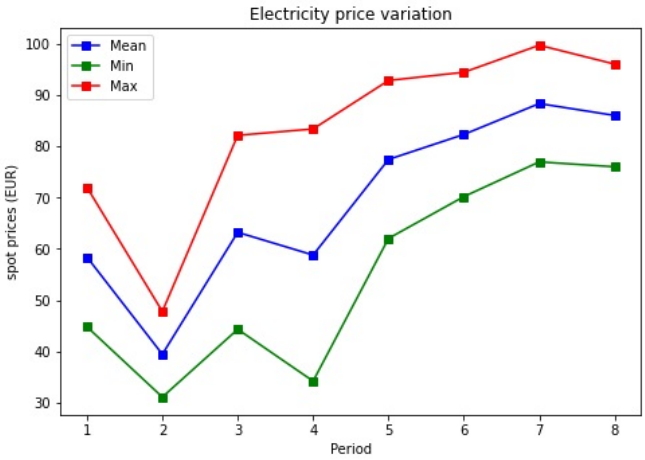

Figure 11. Spot prices in springer day.

4.4.4. Modification of Peak Periods

In this particular scenario, we made a modification to the on-peak period by switching it from t = {5, 6} to t = {4, 7}. This change in the scheduling of on-peak periods had an observable effect on the energy management scheme, as depicted in Figures 12 and 13.

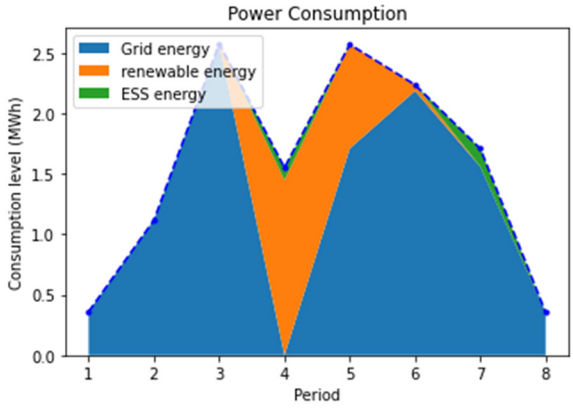

Figure 12. Power consumption for the modified peak periods.

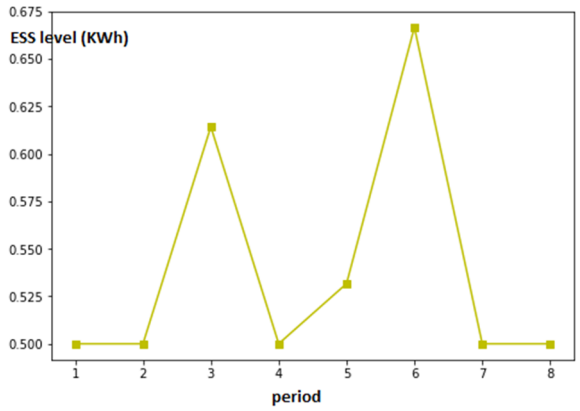

Figure 13. ESS level for the modified peak periods.

Figure 12 illustrates the modified energy consumption pattern in comparison to the benchmark experiment. It is evident that the energy consumption has been altered in the periods t = 4, 5, 6, and 7. Specifically, in the fourth period, the level of energy consumption was approximately 1.5 MWh, which is significantly higher compared to the benchmark

case, where it was 2.5 MWh. This modification in the on-peak period demonstrates the influence of temporal scheduling decisions on energy consumption. By shifting the on-peak periods to t = {4, 7}, there was a noticeable change in energy usage, particularly in the fourth period, where the algorithm accepts a reduction of conventional energy consumption in this periods. The energy requirement in this period is supplied by the renewable energy and the ESS. The decrease in energy consumption during this period indicates a potential optimization opportunity for reducing energy costs or ensuring the efficient utilization of available resources.

The usage of the ESS In this scenario is shown in Figure 13. The ESS is charged in periods t = 3, t = 5, and t = 6 and discharged during the fourth and the seventh periods.

The cost obtained is 519.33, which is slightly lower than the one obtained in the benchmark experiment.

4.4.5. Modification of Budget of Uncertainty

In order to assess the impact of the budget of uncertainty for renewable energy sources, $\Gamma^{(1)}$, we conducted a scenario analysis where we varied its value from zero to eight. This allowed us to examine how changes in the budget of uncertainty influence the performance of the energy management system. Figure 14 shows the sensitivity analysis for $\Gamma^{(1)}$. The x-axis represents $\Gamma^{(1)}$, and the y-axis represents the total cost. The figures demonstrate an increasing trend, suggesting a positive correlation between the two variables. In other words, as the value of $\Gamma^{(1)}$ increases, the total cost increases.

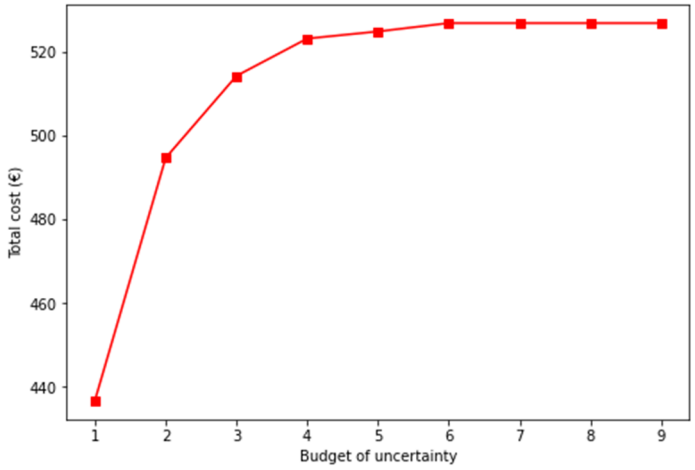

Figure 14. Sensitivity analysis for budget of uncertainty $\Gamma^{(1)}$.

4.5. Verification and Validation of the Decomposition Genetic Approach

To ensure the validity and effectiveness of the proposed decomposition genetic approach, we conducted several computational tests. The objective of these tests was to evaluate and compare the performance of our approach with other algorithms commonly used in production scheduling. Specifically, we assessed the average costs achieved by each algorithm and analyzed the computational time required for their execution.

4.5.1. Instance Generation

To analyze the impact of input parameters on simulation results, we generated nine instances representing different problem sizes. These instances were divided into three classes: small, medium, and large. The instances present the same number of processes. Then, the entire production system is composed of three consecutive processes. The number of items is equal to one for all processes: $|I_p| = 1 \; \forall p \in P$. The number of periods, representing the time horizon for scheduling, varied across the instances. Specifically, we set the number of periods to 6 for the small instance, 24 for the medium instance, and 36 for

the large instance. By adjusting the number of periods, we can observe the impact of time granularity on solar power uncertainty. For the small instance, the mean solar power value for each period was generated randomly from a uniform distribution U(5,24). Similarly, for the medium instance, the range was set to 1 to 7, while for the large instance, it was set to 0.5 to 3. The budget of uncertainty was set to 3 for the small instance, while for the medium instance it was set to 12. Finally, for the large instance, it was set to 18.

The other production parameters, such as demand and capacities, are generated randomly based on [30]. The distinction between each class of instances is based on the varying levels of uncertainty associated with the scheduling horizon. In other words, the difference lies in the extent of unpredictability and variability that exists in the scheduling period. The small instance represents a shorter scheduling horizon, resulting in relatively lower uncertainty. On the other hand, the medium instance encompasses a longer scheduling horizon, leading to increased uncertainty compared to the small instance. Finally, the large instance exhibits the highest level of uncertainty as it involves the longest scheduling horizon among the three classes. By incorporating instances with different levels of uncertainty, we can assess the robustness and performance of our production scheduling model under various scheduling horizons and evaluate its ability to handle different degrees of uncertainty effectively.

4.5.2. Results and Discussion

We tested the proposed approach for three variability levels. Results were compared to the worst-case scenario obtained by the nested Column and Constraint algorithm. Table 5 provides the instance references (S1, S2, S3, M1, M2, M3, L1, L2, L3) along with the corresponding costs and execution times for both the proposed approach and the nested CCG algorithm.

Table 5. Comparison between the proposed approach and the nested CCG algorithm.

	Instance Reference	Proposed Approach Cost (EUR)	Nested CCG Cost (EUR)	Proposed Approach Execution Time (s)	Nested CCG Execution Time (s)
Small	S1	6022.4	6022.4	0.82	2.46
	S2	5817.17	5817.17	0.78	2.38
	S3	5966.83	6049.8	0.81	2.53
Medium	M1	19,874.54	19,934.97	8.86	16.32
	M2	20,136.31	20,193.8	9.32	15.29
	M3	19,797.62	19,812.53	8.81	15.78
Large	L1	31,238.02	32,360.94	28.54	351.29
	L2	29,754.05	30,124.99	29.89	364.87
	L3	31,365.63	31,563.63	28.97	331.13

The comparison of the proposed approach and the nested CCG algorithm, as shown in the last table, reveals some notable insights. Firstly, in terms of cost, the proposed approach consistently achieves similar results in S1 and S2. In this case, the proposed approach found the worst-case scenario related to the solar power generation. In contrast, for the other instances (S3, M1, M2, M3, L1, L2, L3), the proposed approach found costs lower than those found by the nested CCG algorithm. This implies that the proposed approach did not encounter the worst-case scenario in these instances. Instead, it managed to find alternative, more cost-effective solutions. The discrepancy in cost between the two approaches can be attributed to the exponential increase in the search space of the proposed approach as the problem size increases.

Secondly, concerning execution time, the proposed approach outperforms the nested CCG algorithm in terms of speed. It demonstrates significantly shorter execution times for

all instances, suggesting that it is a more efficient algorithm for solving the given problem. Overall, the results highlight the effectiveness of the proposed approach in terms of cost and execution time, making it a favorable choice for addressing the problem at hand.

In developing the proposed production scheduling model, it is important to acknowledge the limitations inherent in its design and application. Firstly, to simplify the complexity of real-world manufacturing processes, certain assumptions were made during the model development. These assumptions include stable production parameters, constant material availability, and reliable equipment performance. These simplifications may not fully capture the dynamic nature and uncertainties present in actual production environments. Moreover, the model's effectiveness is reliant on the availability and quality of data used for parameter estimation and optimization. Inaccurate or limited data may introduce biases and affect the model's performance, potentially leading to suboptimal scheduling decisions or inaccurate cost estimations. Additionally, the scalability of the model should be considered, as solving large-scale optimization problems may pose computational challenges, especially with the presence of binary variables.

5. Conclusions

This study proposes an approach to address the integration of uncertain on-site renewable energy and volatile demand-side management policies into the production scheduling problem for consecutive processes. The manufacturing process in focus relies on multiple energy sources, including the conventional grid, on-site intermittent renewable energy, and an ESS. The approach formulates a two-stage robust mixed-integer linear programming model to evaluate both the economic and environmental performances of incorporating energy-scheduling flexibility. In the first stage, an optimal production schedule is generated to minimize the total production cost. In the second stage, decisions regarding the energy management system are made based on the production schedule to minimize energy costs under the worst-case scenario of renewable energy supply. To solve this complex optimization problem, a decomposition algorithm based on a genetic algorithm is employed. Experiments and sensitivity analysis are conducted using a real case study to assess the effectiveness of the proposed model in generating optimal decisions for the manufacturing system while ensuring flexibility in aligning the production schedule with the renewable energy supply and DSM policies. The numerical results demonstrate that the algorithm can effectively align a near-optimal production schedule with the availability of renewable energy and DSM policies, resulting in reduced production and energy costs as well as decreased CO_2 emissions.

There are several potential avenues for future research in the field of production scheduling and renewable energy integration. These directions can further enhance and expand the proposed model. Firstly, considering the dynamic nature of renewable energy sources, future research can explore the incorporation of real-time data and forecasting techniques to improve the accuracy of renewable energy generation predictions. By integrating advanced forecasting methods, such as machine learning or artificial intelligence algorithms, into the model, more precise estimations of renewable energy availability can be obtained, leading to improved scheduling decisions and cost optimization. Moreover, the proposed model can be extended to incorporate other aspects of sustainable manufacturing, such as the consideration of carbon footprints or other environmental indicators. By integrating environmental objectives into the optimization framework, manufacturers can strive for not only cost reduction but also minimizing their overall environmental impact.

Author Contributions: M.H.J.: conceptualization of this study, methodology, software, acquisition of data, analysis and/or interpretation of data, writing—original draft, writing- review editing. S.M.: conception and design of study, acquisition of data, analysis and/or interpretation of data, writing—original draft, writing—review editing. C.T.: conception and design of study, acquisition of data, analysis and/or interpretation of data, review editing. All authors have read and agreed to the published version of the manuscript.

Funding: This work is supported by Oniris University (France).

Data Availability Statement: The data used are presented in Section 4.

Conflicts of Interest: The author declare no competing interest.

Appendix A

Table A1. Sets and indexes.

Symbol	Description
t	Index for period, t = 1, 2, . . . , |T|
p, p′	Index for processes, p, p′ = 1, 2, . . . , |p|
i	Index for process, i = 1, 2, . . . , $\|I_p\|$
T	Set of time periods in scheduling horizon
P	Set of processes
δ	Set of final processes
θ	Set of batch processes
I_p	Set of items produced by the process p
$\mathbb{N}$	Set of worst-case scenarios
μ_1/μ_2	Set of (on-site renewable energy/spot prices) uncertainty parameters

Table A2. Parameters.

Symbol	Description	Unit
c_p^y	Unit cost per item buffered in process p	EUR
c_t^q	Unit inventory cost at period t	EUR
c_t^v	Unit cost per final product backordered at period t	EUR
$b_{i,p,p'}$	1 if the item i produced by the process p is transmitted to its successor p′, 0 otherwise	-
$D_{i,p,t}$	Demand for final product $o_{i,p}$ at period t, $p \in \delta$	ton
T_p	Cycle time for producing one unit of product at process p	time
α_p	Performance of process p	-
N_p	Buffer capacity of product i for process p	ton
I_{max}	Inventory capacity of finals products	ton
$y0_{i,p}$	The initial intermediate stock level of product i at process p.	ton
$I0_{i,p}$	The initial stock level of final product i at process p, p ∈ δ	ton
K_P	Lot size of batch process p,	ton
f_P	Setup time for batch process p	time
$E_{p,t}$	Power consumed for producing one unit in process p at period t	MW/ton
s_{max}	Maximum storage capacity for the ESS	MWh
s_{min}	Minimum storage capacity for the ESS	MWh
s_0	Initial energy level of the ESS	MWh
R^+/R^-	Charging and discharging capacities of the ESS	MWh
C^+/C^-	Charging and discharging capacities of the ESSESS charging and discharging cost	EUR/MWh
$g_t^{(1)}$	On-site renewable energy price at period t	EUR/MWh
$g_t^{(2)}$	Conventional energy price at period t	EUR/MWh
G_t	Renewable energy available at period t	MW
g_t^+	Incentive received for energy consumption reduction at period t	EUR
$\sigma_t^{(1)}$	Deviation for power generation of on-site renewables at period t	MW
$\sigma_t^{(2)}$	Deviation for spot prices at period t	EUR
$\Gamma^{(1)}$	Budget of uncertainty for on-site renewables availability	-
$\Gamma^{(2)}$	Budget of uncertainty for energy spot prices	-

Table A3. Decision variables.

Symbol	Description
$x_{i,p,t}$	Amount of item i produced in process p at period t
$y_{i,p,t}$	Inventory level of item i in process p at period t
$x^{(1)}_{i,p,p',t}$	Amount of item i produced in process p at period t and transferred to process p′ at period t + 1
$x^{(2)}_{i,p,t}$	Amount of item i produced in process p at period t and buffered at process p at period t
$y^{(1)}_{i,p,p',t}$	Inventory of item i in process p at period t and transferred to process p′ at period t + 1
$y^{(2)}_{i,p,t}$	Inventory of item i in process p at period t and buffered at process p at period t + 1
$q_{i,p,t}$	Inventory level of item i in final process p at period t
$v_{i,p,t}$	Backorder of final product i in process p at period t
$Se_{p,t}$	Binary variable associated to batch process p
s_t	ESS energy level at period t
r^+_t / r^-_t	Amount of power to charge/discharge the ESS at period t
$e^{(2)}_t$	Conventional energy consumed in period t
$e^{(1)}_t$	On-site renewable energy consumed in period t
a_t	Decision of accepting or not energy consumption reduction request at period t
$o^{(1)+}_t / o^{(1)-}_t$	Variables to define availability of renewable energy at period t
$o^{(2)+}_t / o^{(2)-}_t$	Variables to define the spot prices variation at period t

References

1. Ritchie, H.; Roser, M. CO_2 and Greenhouse Gas Emissions. Our World in Data. 2020. Available online: https://ourworldindata.org/co2-and-other-greenhouse-gas-emissions (accessed on 23 March 2023).
2. Gong, X.; Wee, M.V.D.; Pessemier, T.D.; Verbrugge, S.; Colle, D.; Martens, L.; Joseph, J. Energy- and labor-aware production scheduling for sustainable manufacturing: A case study on plastic bottle manufacturing. *Procedia CIRP* **2017**, *61*, 387–392. [CrossRef]
3. Ma, S.; Zhang, Y.; Lv, J.; Ge, Y.; Yang, H. Big data driven predictive production planning for energy-intensive manufacturing industries. *Energy* **2020**, *211*, 118320. [CrossRef]
4. Mohammed, N.A.; Albadi, M.H. Demand response in electricity generation planning. *Electr. J.* **2020**, *33*, 106799. [CrossRef]
5. Albadi, M.H.; El-Saadany, E.F. A summary of demand response in electricity markets. *Electr. Power Syst. Res.* **2008**, *78*, 1989–1996. [CrossRef]
6. Cui, H.; Zhou, K. Industrial power load scheduling considering demand response. *J. Clean. Prod.* **2018**, *204*, 447–460. [CrossRef]
7. Jiang, E.D.; Wang, L. Multi-objective optimization based on decomposition for flexible job shop scheduling under time-of-use electricity prices. *Knowl. Based Syst.* **2020**, *204*, 106177. [CrossRef]
8. Wang, Y.; Li, L. Time-of-use based electricity demand response for sustainable manufacturing systems. *Energy* **2013**, *63*, 233–244. [CrossRef]
9. Ashok, S. Peak-load management in steel plants. *Appl. Energy* **2006**, *83*, 413–424. [CrossRef]
10. Wang, Y.; Li, L. Time of use electricity cost of manufacturing systems: Modeling and monotonicity analysis. *Int. J. Prod. Econ.* **2014**, *156*, 246–259. [CrossRef]
11. Fernandez, M.; Li, L.; Sun, Z. "Just-for-Peak" buffer inventory for peak electricity demand reduction of manufacturing systems. *Int. J. Prod. Econ.* **2013**, *146*, 178–184. [CrossRef]
12. Sun, Z.; Li, L.; Fernandez, M.; Wang, J. Inventory control for peak electricity demand reduction of manufacturing systems considering the tradeoff between production loss and energy savings. *J. Clean. Prod.* **2014**, *82*, 84–93. [CrossRef]
13. Renna, P.; Materi, S. A literature review of energy efficiency and sustainability in manufacturing systems. *Appl. Sci.* **2021**, *11*, 7366. [CrossRef]
14. Wang, S.; Mason, S.J.; Gangammanavar, H. Stochastic optimization for flow-shop scheduling with on-site renewable energy generation using a case in the United States. *Comput. Ind. Eng.* **2020**, *149*, 106812. [CrossRef]
15. Santana-Viera, V.; Jimenez, J.; Jin, T.; Espiritu, J. Implementing factory demand response via onsite renewable energy: A design-of-experiment approach. *Int. J. Prod. Res.* **2015**, *53*, 7034–7048. [CrossRef]
16. Zhai, Y.; Biel, K.; Zhao, F.; Sutherland, J.W. Dynamic scheduling of a flow shop with on-site wind generation for energy cost reduction under real time electricity pricing. *CIRP Ann.-Manuf. Technol.* **2017**, *66*, 41–44. [CrossRef]
17. Golari, M.; Fan, N.; Jin, T. Multistage stochastic optimization for production-inventory planning with intermittent renewable energy. *Prod. Oper. Manag.* **2017**, *26*, 409–425. [CrossRef]
18. Biel, K.; Zhao, F.; Sutherland, J.W.; Glock, C.H. Flow shop scheduling with grid-integrated onsite wind power using stochastic MILP. *Int. J. Prod. Res.* **2018**, *56*, 2076–2098. [CrossRef]

19. Duarte, J.L.R.; Fan, N.; Jin, T. Multi-process production scheduling with variable renewable integration and demand response. *Eur. J. Oper. Res.* **2020**, *281*, 186–200. [CrossRef]
20. Materi, S.; D'Abgola, A.; Renna, P. A dynamic decision model for energy-efficient scheduling of manufacturing system with renewable energy supply. *J. Clean. Prod.* **2020**, *270*, 122028. [CrossRef]
21. Ben-Tal, A.; El chaoui, L.; Nemirovski, A. *Robust Optimization*; Princeton University Press: Princeton, NJ, USA, 2009.
22. Alem, D.; Curcio, E.; Amorim, P.; Almada-Lobo, B. A computational study of the general lot-sizing and scheduling model under demand uncertainty via robust and stochastic approaches. *Comput. Oper. Res.* **2018**, *90*, 125–141. [CrossRef]
23. Melgar Dominguez, O.D.; Pourakbari-Kasmaei, M.; Mantovani, J.R.S. Adaptive robust short -term planning of electrical distribution systems considering siting and sizing of renewable energy-based DG units. *IEEE Trans. Sustain. Energy* **2019**, *10*, 158–169. [CrossRef]
24. Zeng, B.; Zhao, L. Solving two-stage robust optimization problems using a column-and-constraint generation method. *Oper. Res. Lett.* **2013**, *41*, 457–461. [CrossRef]
25. Herrmann, J.W. A genetic algorithm for minimax optimization problems. In Proceedings of the 1999 Congress on Evolutionary Computation-CEC99, Washington, DC, USA, 6–9 July 1999.
26. Taghikhani, M.A. Renewable resources and storage systems stochastic multi-objective optimal energy scheduling considering load and generation uncertainties. *J. Energy Storage* **2021**, *43*, 103293. [CrossRef]
27. Rahman, H.F.; Sarker, R.; Essam, I. A genetic algorithm for permutation flow shop scheduling under make to stock production system. *Comput. Ind. Eng.* **2015**, *90*, 12–24. [CrossRef]
28. Tecaliman. Available online: https://www.tecaliman.com/ (accessed on 1 June 2023).
29. Guo, Y.; Zhao, C. Islanding-aware robust energy management for micro-grids. *IEEE Trans. Smart Grid* **2018**, *9*, 1301–1309. [CrossRef]
30. Özdamar, L.; Barbarasoglu, G. Hybrid heuristics for the multi-stage capacitated lot sizing and loading problem. *J. Oper. Res. Soc.* **1999**, *50*, 810–825. [CrossRef]

Disclaimer/Publisher's Note: The statements, opinions and data contained in all publications are solely those of the individual author(s) and contributor(s) and not of MDPI and/or the editor(s). MDPI and/or the editor(s) disclaim responsibility for any injury to people or property resulting from any ideas, methods, instructions or products referred to in the content.